Web: www.witpress.com Email witpress@witpress.com
Paper from: *Coastal Environment,* CA Brebbia (Editor).
ISBN 1-85312-921-6

Laboratory investigation of sediment resuspension by waves at full-scale

J. J. Williams, P. S. Bell & K. F. E. Betteridge
Proudman Oceanographic Laboratory, Bidston Observatory, UK.

Abstract

Measurements of wave-induced flows, suspended sediments and bedforms have been obtained in random wave conditions in a large laboratory wave flume over beds of fine and medium sand. Selected results illustrating wave-induced flows and turbulence, bedform genesis and development, sediment resuspension and vertical suspended sediment concentration profiles are presented and are compared with existing empirical formulae and models.

1 Introduction

Due to advances in acoustic technology over the past decade, it is now possible to obtain detailed, approximately co-located intra-wave measurements of wave-induced flows and turbulence, sediment resuspension and bedforms. The study described here follows on from investigations undertaken by the present research consortium in the Deltaflume to quantify local modification to processes by a large benthic tripod [1]. The objectives of the present study are to build upon the existing data base and to verify and quantify characteristics of oscillatory sediment transport processes at full-scale. The experiments reported here focus upon sediment resuspension processes by random waves and the dynamic interactions occurring between waves, bedforms and suspended sediments.

2 Measurements

Measurements were made in the Delft Hydraulics Laboratory Deltaflume (230 m long, 5 m wide and 7 m deep). The facility has a capacity to generate regular and irregular waves with a height up to 2 m, thereby permitting the study of

Paper from: *Coastal Environment*, CA Brebbia (Editor).
ISBN 1-85312-921-6

wave phenomenon at virtually field-scale. Measurements were obtained above beds of sand comprising in test series M, medium sand (D_{50} = 0.349 mm), and in test series F, fine sand (D_{50} = 0.220 mm), Figure 1. The sandy beds, approximately 30 m long, 5 m wide and 0.75 m deep, were placed in the flume, carefully levelled and then compacted (Figure 2a).

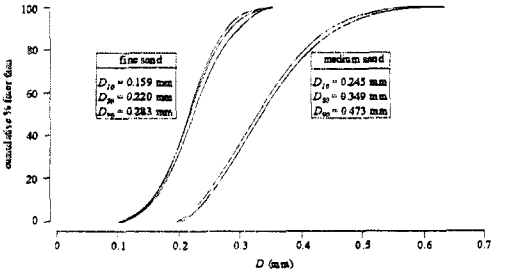

Figure 1: Test sediment grain size distributions instruments.

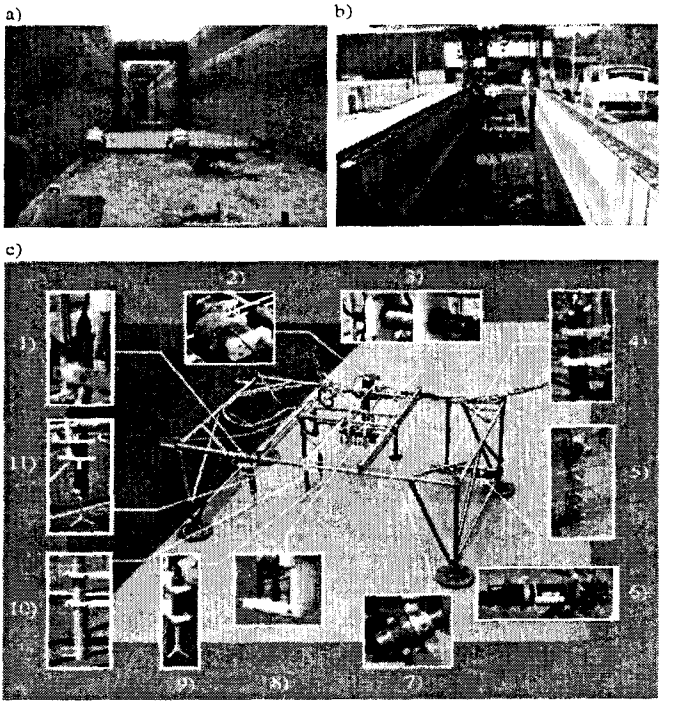

Figure 2: Deltaflume and POL frame: a) emplacement and levelling of the medium sand bed; b) deployment of the POL frame; c) POL frame and instruments showing 1) pressure sensor, 2) stepper motor and chain drive, 3) ARP, 4) SSS, 5) ECMs, 6) LISST, 7) 3-D Doppler, 8) ABS, 9) ADV-1, 10) pump sampling nozzles, 11) ADV-2.

Paper from: *Coastal Environment*, CA Brebbia (Editor).
ISBN 1-85312-921-6

Equipment deployed in the Delta flume comprised a frame and a suite of approximately co-located sensors and sampling devises, (Figure 2b & 2c). Instrument and data logging technologies developed for the benthic frames STABLE [2] and PIP [3] was modified for use in the present study. To allow instruments to be positioned at a required location above the bed the main instrument carriage could be driven forwards or backwards by means of a stepper motor and chain drive. All instrument data logging systems were synchronised and as far as practicable all data were logged at 16 Hz. In addition to the frame, measurements of the water surface elevation were obtained at three locations and wave-induced flows were measured at 5 heights above the bed by electromagnetic current meters, ECMs on the side-wall of the flume (Figure 2c).

Instruments on the frame to measure waves and wave-induced flows (Figure 2c) comprised a pressure sensor, PS, an acoustic Doppler velocimeters, ADV-1 & ADV-2, and a 3D Coherent Doppler Velocity Profiler, 3D-Doppler (vertical resolution = 4.6 cm over the range 0 cm < z < 80 cm). Estimates of velocity v were obtained from the 3D-Doppler using

$$v = \frac{cf_d}{2f_o} \tag{1}$$

where c is the speed of sound in water, f_d is the Doppler frequency and f_o is the transmit frequency [4]. Two additional receivers scanning the insonnified volume enabled measurements of orthogonal turbulent flow components. Transmit-receive frequency was 524 kHz with sound pulses emitted at a rate of 512 kHz and lasting 61 μs. Return signals were range-gated in time corresponding to bin length and required distance from the transducer [5]. Instruments to measure the vertical suspended sediment concentration profiles, C-Profiles, and to obtain samples of suspended sediment comprised a triple frequency (1.0 MHz, 2.0 MHz and 4.0 MHz) acoustic backscatter system, *ABS*, [6] and pump-sampling equipment [7]. Data from the *ABS* were smoothed using a 32 point block online average to give data with 0.25 s resolution. This effectively reduced configurational noise resulting from a random phase distribution of echoes, [8]. Suspended sediment concentration, C, was then computed using

$$C = \frac{\chi^2}{\frac{\chi_o^2}{C_o} - \int_{r_o}^{r} 4\Delta\chi^2 dr} \tag{2}$$

$$\chi = \left(\frac{\Pr\psi}{K_s}\right) e^{2ra_w} \tag{3}$$

such that at range r_o, $C_o = C(r_o)$ and $\chi_o = \chi(r_o)$. The parameters K_s and Δ depend on particle size a_s and the concentration C_o at range r_o is given by the pump sample. Information pertaining to particle size distribution with height was obtained using the Bernoulli solution described by [9]. The bed morphology in a circular area of radius approximately 5 m was measured beneath the POL frame at 1 minute intervals using high-resolution sector-scanning sonar, SSS, consisting of a small, fan beam acoustic transducer mounted on a stepper motor

Paper from: *Coastal Environment*, CA Brebbia (Editor).
ISBN 1-85312-921-6

[10]. In addition, an acoustic ripple profiler, ARP, consisting of a 2MHz transducer mounted onto a motor [11], was used to measure the morphology of the bed at approximately 30 s intervals along a single line of length approximately 4 m centred beneath the POL frame and running along the x axis.

3 Data analysis

In a series of tests the peak wave period, T_p, was held constant at 6 s, and the significant wave height, H_s, was progressively raised in steps and then reduced to the starting value for each sand bed (Table 1). For each test, measurements were obtained for 60 minutes by which time changes in bed morphology were no longer observed.

Table 1: Wave conditions used in tests on the medium and fine sand beds.

Fine sand	T_p	H_s	Medium sand	T_p	H_s
F01_2	6	0.3	M02_2	6	0.4
F02_1	6	0.4	M03_2	6	0.5
F03_1	6	0.5	M04_2	6	0.6
F04_1	6	0.6	M05_2	6	0.8
F05_1	6	0.8	M06_2	6	1.0
F06_2	6	1.0	M07_2	6	1.2
F07_2	6	1.2	M08_2	6	1.4
F08_2	6	1.4	M09_2	6	1.6
F09_2	6	1.3	M10_2	6	1.8
F10_2	6	1.2	M11_2	6	1.6
F11_2	6	1.1	M12_2	6	1.4
F12_2	6	1.0	M13_2	6	1.2
F13_2	6	0.8	M14_2	6	1.0
F14_2	6	0.6	M15_2	6	0.8
F15_2	6	0.4	M16_2	6	0.6
F16_2	6	0.3	M17_2	6	0.4

The pressure sensor data were corrected for depth-attenuation using linear wave theory [12] before converting into time-series of water depth, h. The ABS instruments were calibrated using *in situ* pump-samples eqns (2 & 3). Laboratory tests were used to provide calibration information necessary to process the SSS and ARP data. Manufacturers' calibrations and software were used for the ADV instruments [13]. Being reliant upon a measured shift in frequency eqn (1), the 3D-Doppler instrument required no special calibration [5]. The orthogonal turbulent flow components measured by the ADVs and the 3D-Doppler were then correct for slight misalignment in the vertical and horizontal planes using an axes rotation algorithm [14] and corrected zero-mean flow component time-series u, v and w, comprising wave-induced fluid motion were calculated.

In order to investigate turbulence, wave-induced fluid motion was removed

Paper from: *Coastal Environment*, CA Brebbia (Editor).
ISBN 1-85312-921-6

effectively from the u, v and w time-series using a moving average, MA, filter in the form

$$F_{j(t+1)} = \frac{1}{N}\sum_{j=1}^{N} A_{t-j+1} \tag{6}$$

where F_j is the forecasted value at time j, N is the number of prior periods to include in the MA and A_j is the actual value at time j. Parameter values in eqn (6) were chosen to give 1 s average values of u, v and w and the resulting 1 Hz MA series comprising wave motion, u_w, v_w and w_w were then re-sampled at the original sampling frequency and subtracted from the original signal to obtain the time-series u_t, v_t and w_t comprising principally turbulence. The RMS wave-induced flow speed was then calculated from $\overline{U}_w = (\overline{u}_w^2 + \overline{v}_w^2)^{0.5}/\sqrt{2}$. Further details of data analysis are given by [1].

4 Results and discussion

Time-series, spanning 80 s during test M07_2, of surface elevation, h, and wave-induced flow components u and w measured by the ECMs and the ADV-1 are shown in Figure 3a. In accord with linear theory the amplitude of u and w time-series are shown to increases gradually with distance above the bed. Close to the bed, u and w time-series measured by the ADV indicate the presence of turbulence. To examine the scales of turbulent motion resolved by the flow sensors, power spectra and co-spectra of u, v and w measured by the ADV-1 and ADV-2 at $z \approx 14$ cm and $z \approx 57$ cm, respectively, and u and w measured by a Delft ECM at $z \approx 25$ cm during test M07_2 are shown in Figure 3b. Here Fourier amplitudes, $A_x(n)$, were computed over a range of frequencies, f, defined by the sampling interval, Δt, and the record length, n, using an FFT algorithm, where x is u, v or w. The 1-dimensional power spectra were then computed and scaled using $S_x(n) = A_x(n).A_x*(n)$, where * indicates a complex conjugate. The spectra for u and co-spectra uw show a characteristic wave peak centred around f = 0.17 Hz (T = 6 s) and exhibit approximately anisotropic behaviour in the range $10^{-2} < f < 10^{0}$ with $Su_t(n)$ larger than $Sv_t(n)$ and $Sv_t(n)$ larger than $Sw_t(n)$. This behaviour typifies the region of turbulent energy production in a shear flow. For $f > 10^{0}$, spectra for the ECM and ADV diverge. This is attributable both to the smaller sampling volume of the ADV and thus its ability to resolve small-scale turbulence and to the difference in sensor heights above the bed. Williams et al. [1] show that turbulence due to the presence of the frame is not detected in this near-bed region. Figure 3c shows 5 time-series spanning 60 s of u and w measured by the 3D-Doppler from a location close to the bed to $z \approx 25$ cm at intervals of 4.6 cm. An increase in the amplitude of the wave-induced fluid motion is clearly seen as is an enhancement of turbulence associated with a group of waves.

The ability to position instruments on the carriage at known locations relative to measured bed morphology has allowed investigation of spatial changes in

Paper from: *Coastal Environment,* CA Brebbia (Editor).
ISBN 1-85312-921-6

turbulence production and the vortex ejection mechanism. In addition, measurements from the 3D-Doppler are giving new insight into the near bed flow regime above rippled beds and in sheet flow conditions and are providing a means of examining phase relationships between near-bed wave-induced flows and sediment resuspension events up to 0.5 m above the bed.

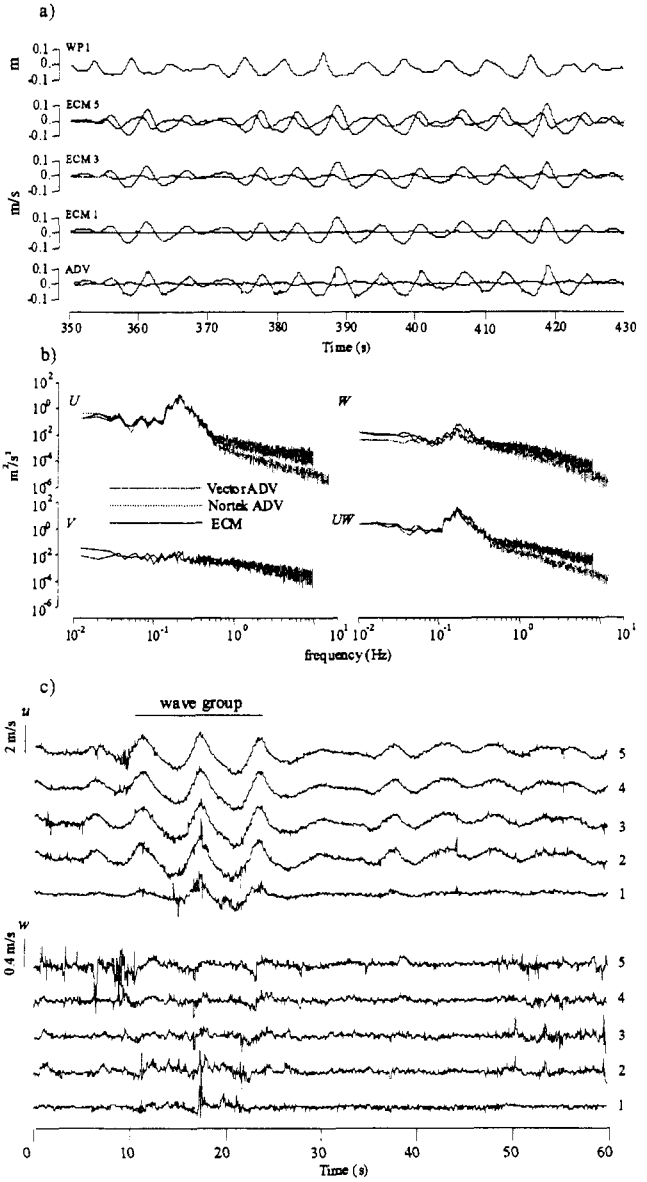

Figure 3: a) Measured waves and wave-induced currents and b) power spectra and co-spectra of flow components measured by the ADVs and ECM.

Paper from: *Coastal Environment,* CA Brebbia (Editor).
ISBN 1-85312-921-6

Bed profiles measured by the ARP at the end of each 60 minute test, showing ripples on the medium and fine sand beds, are illustrated in Figure 4. In the case of the medium sand in Figure 4a, a clear sequence of ripple development is shown. In low wave conditions the ripples are regular and small. As wave height increases to a maximum value during test M10_2, the ripple height, h_r, and wavelength, λ_r, also increase to their maximum size. Whilst a subsequent reduction in wave height reduces both h_r, and λ_r values, they are found to exhibit hysteresis and do not return to the values observed at the start of the experimental series. The pattern of ripple development on the fine sand bed is rather different. Figure 4b shows an initial increase in both h_r, and λ_r values in response to increased wave height. However, around test F06_2, h_r, and λ_r values decrease in response to increasing wave height before again decreasing around test F11_2 as the wave height again decreases.

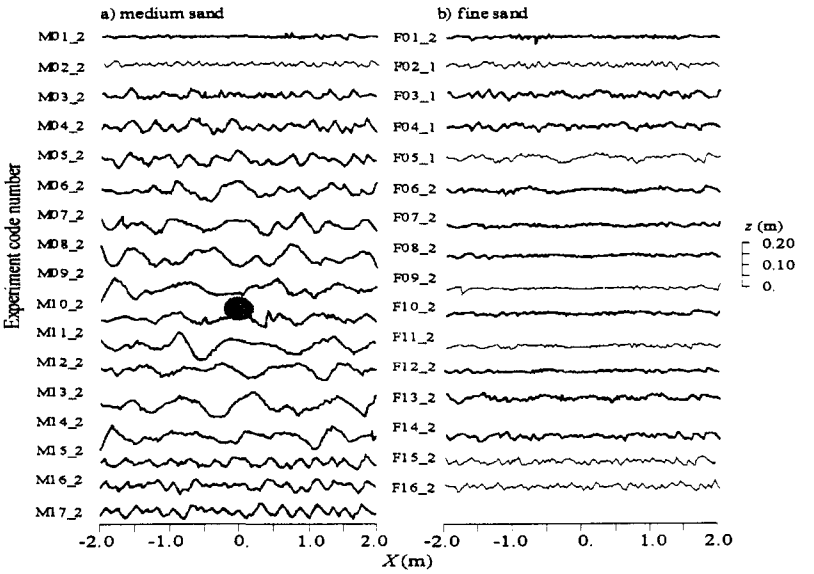

Figure 4: Bed profiles measured by the ARP at the end of tests on the medium and fine sand beds.

Whilst Figure 4 indicates a relationship between ripple geometry and H_s, further analysis of ARP profiles by zero down-crossing and wavelet analyses [1, 15] revealed significant variability in both h_r and λ_r in time and space. It was noted that most modification to ripple geometry occurred during the first 30 minutes of a given test in response to either an increase or decrease in H_s. Thereafter, for the next 30 minutes, temporal and spatial changes in the height and wavelength of ripples were less evident. Figure 5 shows analysis of 29 ARP profiles measured during the last 30 minutes of tests on the medium and fine sand beds. Also shown are H_s values for each test presented. The statistical

Paper from: *Coastal Environment,* CA Brebbia (Editor).
ISBN 1-85312-921-6

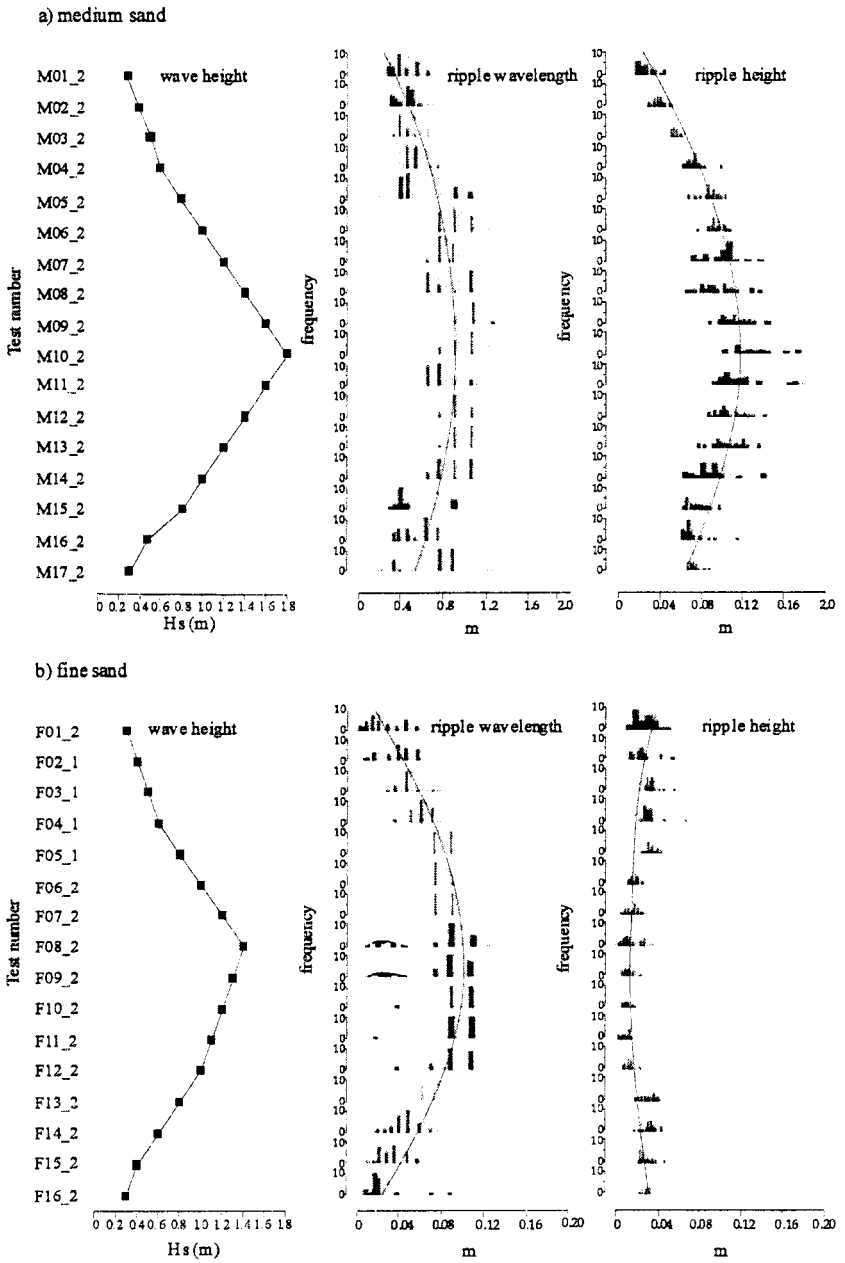

Figure 5: Measured wave height, ripple wavelength and ripple height for tests on the medium and fine sand beds.

distributions of h_r and λ_r values are presented as histograms. Also shown by the solid line are median values and scaled normal probability density functions

Paper from: *Coastal Environment*, CA Brebbia (Editor).
ISBN 1-85312-921-6

spanning the range of observed values. As demonstrated by Figure 4, Figure 5a shows that in the case of the medium sand, h_r and h_r and λ_r values increase in response to an increase in H_s and subsequently decline as wave height reduces. Whilst a similar response is shown in Figure 5b for λ_r values on the fine sand bed, h_r values show the opposite response with minimum values attained at the maximum H_s value. In this case the value of the wave mobility number, ψ, $= U_w^2 / g(s-1)D_{50}$, where U_w is the wave orbital velocity, exceed a critical value for ripple development in the present water depth around $H_s \approx 1.0$ m and the bed regime enters a transitional phase before the onset of sheet flow around $H_s \approx 1.2$ m [16]. However, the persistence of low amplitude, relatively long wavelength bedforms shows clearly that the onset of sheet flow is not accompanied by flattening of the bed. Figure 5b shows also a bi-modal distribution of λ_r values on the fine sand bed at H_s value around 1.4 m with peaks in wavelength $O(0.2$ m) and $O(1.0$ m) observed.

For regular laboratory waves [17] expresses ripple geometry in terms of the wave mobility number, ψ, $= U_w^2 / g(s-1)D_{50}$, where U_w is the wave orbital velocity for monochromatic waves, s is the ration of densities of grains to water (1.65) and the skin friction Shields parameter, θ_{ws}, $= \tau_{ws} / g(\rho_s - \rho)D_{50}$ in the form $h_r = A(0.275 - 0.022\psi^{0.5})$ and $\lambda_r = h_r/(0.182 - 0.24\theta_{ws}^{1.5})$, for $\psi < 156$ and $\theta_{ws} < 0.831$, respectively. Values of the skin friction bed shear stress, τ_{ws}, were computed from $\tau_{ws} = 0.5\rho f_w U_w^2$, where the smooth bed friction factor, f_w is given by $f_w = -1.39(A/0.083D50)^{-0.52}$ and the orbital amplitude, $A = U_w T/2\pi$. For irregular wave condition pertaining during the present tests, [1] gives the equations

$$h_r = 21A\psi^{-1.85} \tag{7}$$

$$\lambda_r = A\exp[(693 - 0.37\{\ln\psi\}^8)/(1000 + 0.75\{\ln\psi\}^7)] \tag{8}$$

where the parameters A and U_w relate to the significant wave height. Comparisons between measured and predicted h_r and λ_r values are shown in Figure 6. Whilst as expected there reasonable agreement between measured and predicted λ_r values for random waves, the predicted h_r values in random waves deviate greatly from the measured values. In this case, better correlation is found between measured h_r values and h_r values predicted for regular wave conditions. The resuspension of fine bed sediments by the combined action of single waves and groups of larger than average waves is shown in Figure 7 which shows time-series spanning 180 s of u_w, h, u_t, w_w, w_t and an image of the suspended sediment concentration field measured by the 2 MHz ABS instrument for 0 cm $< z <$ 100 cm. Here arrows are used to demonstrate the temporal correlations between individual waves and sediment resuspension events. Also shown are two resuspension 'clouds' that grow in height and persist for at least 20 s after passage of a wave group. The resuspension clouds shown in Figure 7 extend up to 80 cm above the bed and show evidence of the wave pumping process associated with groups. Figure 7 shows the high resolution of resuspension processes and associated hydrodynamics now made possible with acoustic

Web: www.witpress.com Email witpress@witpress.com
Paper from: *Coastal Environment,* CA Brebbia (Editor).
ISBN 1-85312-921-6

instruments and reveals a level of complexity not yet considered by numerical models.

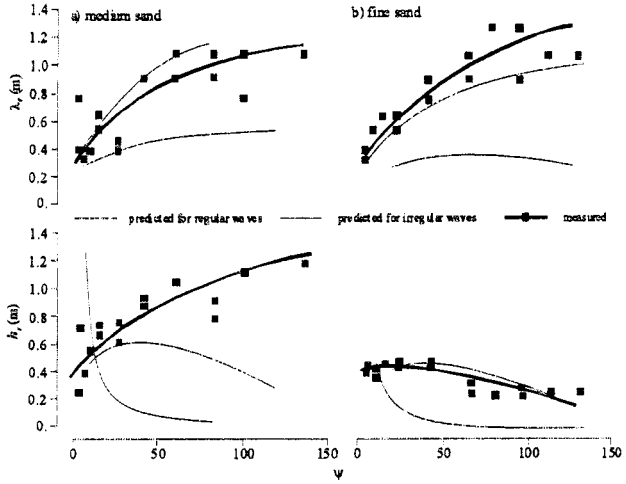

Figure 6: Comparison between measured and predicted ripple height and wavelength in regular and irregular waves on the medium and fine sand bed.

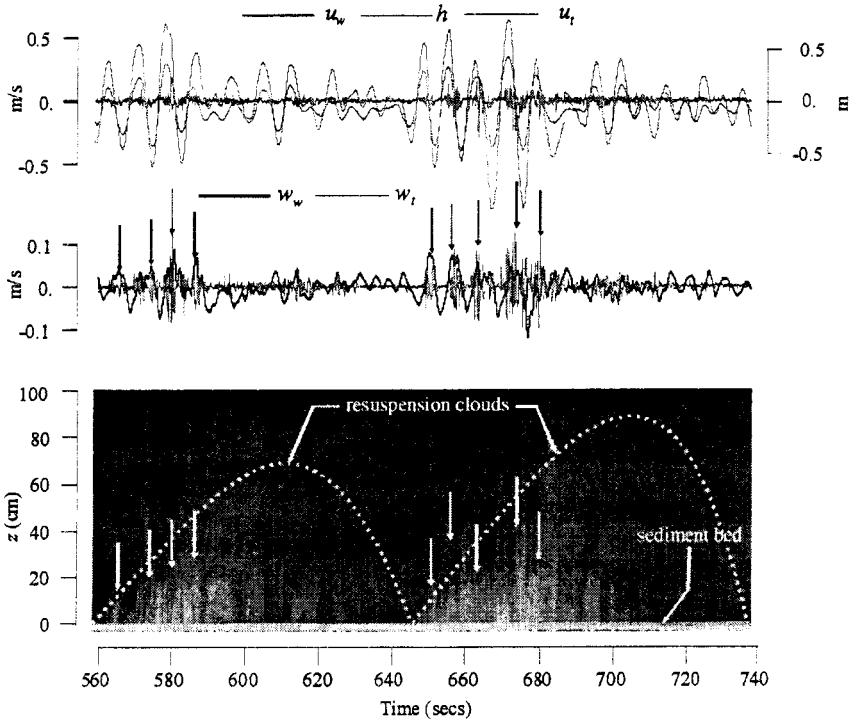

Figure 7: Resuspension of fine bed sediment by combined action of single waves and wave groups.

Paper from: *Coastal Environment*, CA Brebbia (Editor).
ISBN 1-85312-921-6

Examples of C-profiles, measured during tests on the medium and fine sand beds by pump-sampling, are shown in Figure 8a. For a given test bed this figure shows clearly that despite the wide range of test wave conditions, C-profiles are similar in shape and magnitude and exhibit and approximately exponential decay with z. Relationships between C-profiles, wave-induced flows and bed morphology are the subject of on-going research. Figure 8b shows a comparison between C-profiles measured by pump-sampling and by the 2 MHz ABS for tests M04_1 (H_s = 0.6 m) and M07_1 (H_s = 1.2 m).

For wave-only conditions C-profiles usually conform to $C(z) = C_0 e^{-z/l}$, where C is the suspended sediment concentration (m^3/m^3) at height z, C_0 is the reference concentration (m^3/m^3) at the sea bed (m^3/m^3) and l is a decay length scale. For the present tests, $l = 1.4\lambda_r$, $C_0 = 0.005\theta_r^3$, $\theta_r = f_w U_w^2 / 2(s-1)gD_{50}(1-\pi h_r/\lambda_r)^2$, $f_w = 0.00251\exp(5.21r^{-0.19})$ and $r = U_w T / 5\pi D_{50}$. Predicted C-profiles are compared with measured C-profiles in Figure 8b and show good agreement in the range 0.01 m < z < 0.3 m.

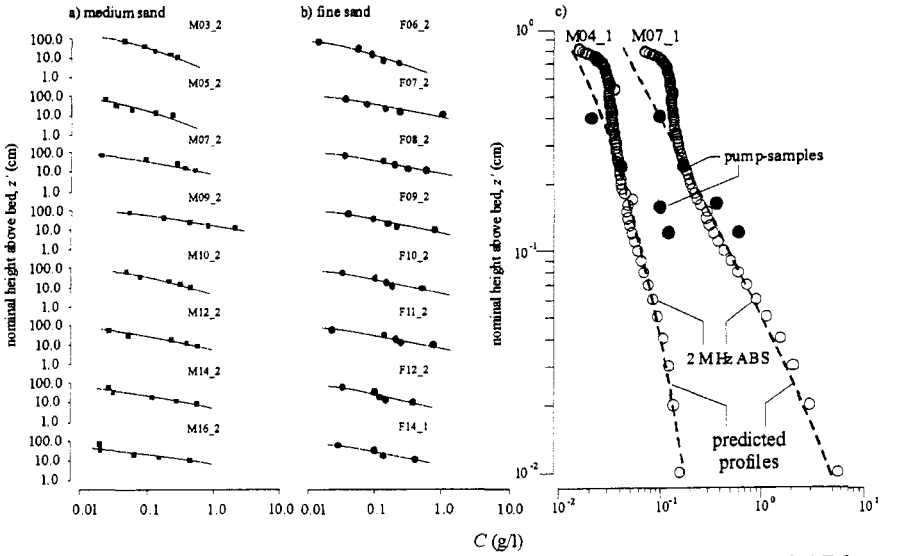

Figure 8: Measured suspended sediment concentration profiles (pump and ABS).

5 Conclusions

Measurements obtained using state-of-the-art instruments deployed using a specially designed frame in a large laboratory wave flume have provided new insight into the processes of sediment resuspension and bedform development. Specifically, these data allow investigation of the dynamic feedback occurring between bedforms and sediment entrainment mechanisms and of the changes in near-bed hydrodynamics conditions and sediment dynamics occurring during the transition from a rippled regime to sheet flow conditions. The present systematic investigation of bed response to changing hydrodynamic forcing has wider

Paper from: *Coastal Environment*, CA Brebbia (Editor).
ISBN 1-85312-921-6

applications in aiding parameterisation of numerical models of coastal systems which must consider the relationship between the present bed morphology and antecedent wave conditions. It is helpful also in investigation of the dynamic feedback linking hydrodynamics, suspended sediments and bed morphology in natural situations.

Acknowledgements

The work was jointly supported by the European Communities through the Access to Research Infrastructure Action of the Improving Human Potential Programme and by the Natural Environment Research Council.

References

[1] Williams J. J., Bell P. S., Thorne P. D., Trouw K., Hardcastle P. J. & Humphery J. D. Observed and Predicted Vertical Suspended Sediment Concentration Profiles and Bedforms in Oscillatory-Only Flow. Journal of Coastal research, **16**(3), 698-708, 1999a.

[2] Humphery J. D. & Moores S.P., STABLE II - An improved benthic lander for the study of turbulent wave-current-bed interactions and associated sediment transport. *Electronic Engineering in Oceanography*, IEE Conference Publication No. **394**, 170-174, 1994.

[3] Williams J. J., Bell P. & Thorne P. D., Field measurements of flow fields and sediment transport above mobile bedforms. *Journal of Geophysical Research* (in review), 2002.

[4] Zedel L. & Hay A. E., A coherent Doppler Profiler for High-Resolution Particle Velocimetry in the Ocean: Laboratory Measurements of Turbulence and Particle Flux. *Journal of Atmospheric and Oceanic Technology.*, 16, 1102-1117, 1999.

[5] Betteridge K. F. E., Thorne P. D. & Bell P.S., Assessment of acoustic coherent Doppler and cross-correlation techniques for measuring near-bed velocity and suspended sediment profiles in the marine environment. *Journal of Atmospheric and Oceanic Technology* (in review), 2002.

[6] Thorne P. D. & Hardcastle P. J., Acoustic measurements of suspended sediments in turbulent currents and comparison with *in-situ* samples. *Journal of the Acoustic Society of America*, **101**(5), 2603-2614, 1997.

[7] Bosman, J. J., Velden, E. T. J. M. Van Der, Hulsbergen C. H., Sediment concentration measurements by transverse suction. *Coastal Engineering*, **11**, 353-370, 1997.

[8] Thorne P. D., Hardcastle P. J. & Soulsby R. L., Analysis of acoustic measurements of suspended sediments. *Journal of Geophysical Research*, **98**(C1), 899-910, 1993.

[9] Lee T. H. & Hanes D. M., Direct inversion method to measure the concentration profile of suspended particles using backscattered sound. *Journal of Geophysical Research*,**100**(C2), 2649-2657, 1995.

Paper from: *Coastal Environment,* CA Brebbia (Editor).
ISBN 1-85312-921-6

[10] Bell P. S., Thorne P. D. & Williams J. J., Acoustic measurements of sand ripple profile evolution under controlled wave conditions. *4th International Conference on Underwater Acoustics*, A. Alippi & G. B. Cannelli, Eds. Rome, Italian National Research Council, Vol. 1, 353-358, 1998.

[11] Bell P. S., Thorne P. D., Measurements of sea bed ripple evolution in an estuarine environment using a high resolution acoustic sand ripple profiling system. *Oceans '97*, Volume 1, MTS/IEEE, Washington D.C., pp. 339-343, 1997.

[12] Bishop C. T. & Donelan M. A., Measuring waves with pressure transducers. *Coastal Engineering*, **11**, 309-328, 1997.

[13] Voulgaris G. & Trowbridge J. H., Evaluation of the acoustic Doppler velocimeter (ADV) for turbulence measurements. *Journal of Atmospheric and Ocean Technology*, **15**, 272-289, 1998.

[14] Hannay A., Williams J. J., West J. R. & Coates L. E., A field study of wave: current interactions over a rippled sandy bed. *EUROMECH 310: Sediment Transport Mechanisms in Coastal Environments and Rivers*, M. Belorgey, R. D. Rajaona & J. A. F. Sleath (editors), World Scientific, 345-359, 1994.

[15] Torrence C. & Compo G. P., A Practical Guide to Wavelet Analysis. *Bulletin of the American Meteorological Society*, **79**, 61-78, 1998.

[16] Soulsby R. L., *Dynamics of marine sands: a manual for practical applications*. Thomas Telford Publications, 249pp, 1997.

[17] Nielsen P., *Coastal Bottom Boundary Layer and Sediment Transport.* World Scientific, River Edge, N. J., USA, 1992.